



ISSN: 2230-9926

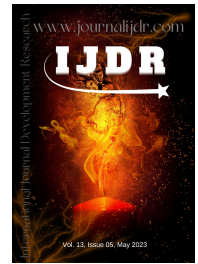
Available online at <http://www.journalijdr.com>

IJDR

International Journal of Development Research

Vol. 13, Issue, 05, pp. 62559-62568, May, 2023

<https://doi.org/10.37118/ijdr.26547.05.2023>



RESEARCH ARTICLE

OPEN ACCESS

DEVELOPMENT OF STEEL FOR HOT STAMPING OF 22MnB5 STEEL BY JOULE EFFECT HEATING

Julio Henrique Pimentel Medrano^{*1,4}, José Eduardo Ribeiro de Carvalho², Carlos Angelo Nunes^{3,4} and Tatiane Caroline Ferrari⁵

¹Metallurgist Engineer, M.Sc. in Mechanical Engineering, IST Senai Metal Mecânica, Maringá-PR, Brazil; ²Metallurgist Engineer, M.Sc. in Metallurgical Engineering, CSN, Volta Redonda-RJ, Brazil; ³Metallurgist Engineer, M.Sc. in Mechanical Engineering, PhD in Mechanical Engineering, University of São Paulo, USP EEL, Lorena-SP, Brazil; ⁴Graduate Program in Materials Engineering, University of São Paulo, USP EEL, Lorena-SP, Brazil; ⁵Chemical Engineer, Postdoctoral student in Chemical Engineering, Postgraduate Program in Chemical Engineering, Federal University of Paraná, Curitiba – PR, Brazil

ARTICLE INFO

Article History:

Received 11th March, 2023

Received in revised form
20th April, 2023

Accepted 16th April, 2023

Published online 24th May, 2023

KeyWords:

Hot Stamping, Steel, Boron.

*Corresponding author:

Julio Henrique Pimentel Medrano

ABSTRACT

With the increase in demand and development of the automobile sector, where it becomes important to improve the efficiency of energy consumption of vehicles, one can observe the need for materials that are both light and have high mechanical strengths. The Ultra High Strength Steel (UHSS), which include TWIP (Twinning-Induced-Plasticity) and Hot Stamping are characterized by unique microstructures and metallurgical properties that allow car manufacturers to meet the diverse functional requirements of vehicles. Boron steel is suitable for mechanical hot forming. In the last few years, hot stamped parts have occupied a prominent place in the bodies of bodies due to being in line with the demands mentioned above. There is a lot of research under development for this technology, be it in materials, means of production, coatings and applications. Currently, there is a patent that generates a technological restriction for the processing of hot stamping; in which it is to use boron steel with Al-Si metallic coating and heating the blank to be hot stamped through a radiation furnace. The objective of this work is to use a new processing alternative through another metallic diffusion coating of Fe-Zn and heating of the blank to be hot stamped by Joule effect; generating an industrial experiment and prototyping for characterization. The results showed the feasibility of using boron steel with Fe-Zn diffusion coating in hot forming applications by heating by Joule effect, with good surface quality, meets the mechanical properties and microstructure, without cracks in the steel, excellent adhesion of the paint layer and good resistance to corrosion.

Copyright©2023, ZAPJI YMELE Aime Philombe et al. This is an open access article distributed under the Creative Commons Attribution License, which permits unrestricted use, distribution, and reproduction in any medium, provided the original work is properly cited.

Citation: Julio Henrique Pimentel Medrano, José Eduardo Ribeiro de Carvalho, Carlos Angelo Nunes and Tatiane Caroline Ferrari. 2023. "Development of steel for hot stamping of 22MnB5 steel by joule effect heating". *International Journal of Development Research*, 13, (05), 62559-62568.

INTRODUCTION

Galvanizing Line: Currently, much attention has been paid to the development of galvanized coatings for boron steel intended for hot stamping, particularly with Fe-Zn diffusion coating, due to its surface quality at the end of the process, the galvanic protection it provides to the parts and the ease of adapting industrial galvanizing lines to your production. However, the challenges are enormous, mainly that of guaranteeing the structural integrity of the layer containing Zn after the hot stamping process, since the temperatures involved are higher than the melting point of Zn and not detecting cracks in boron steel (NAKANO et al., 2015; CUI et al., 2012). There are several types of surface treatments for steel, among which zinc plating, chrome plating, nickel plating and tin plating are some examples. The diffusional Fe-Zn coating is a differentiator (DRILLET et al., 2011;

IKEUCHI and YANAGIMOTO et al., 2011). The continuous galvanizing line studied is of the Dual Purpose type, which receives this name, as it has the purpose of producing cold-rolled steel sheets and hot-dip galvanized steel sheets, in addition to steel sheets for stamping and high-strength steel that is solid-solution-hardened and dual-phase structure, alternating routes in a single processing line. It has 5 processing sections, which are: entry section, pre-treatment section, process section – furnace and coating, post-treatment section and output section. In general terms, it has the following equipment: unwinding machine, annealing oven, a liquid metal pot, air jet coating system, pre-melting pot, surface hardening laminator and tension leveler, in addition to a roll-coater for applying chemical post treatment products, vertical and horizontal inspection cabin, electrostatic oiler and winder. Table 1 shows the technical characteristics of the continuous galvanizing line studied (JEON et al., 2015; JIAN et al., 2015).

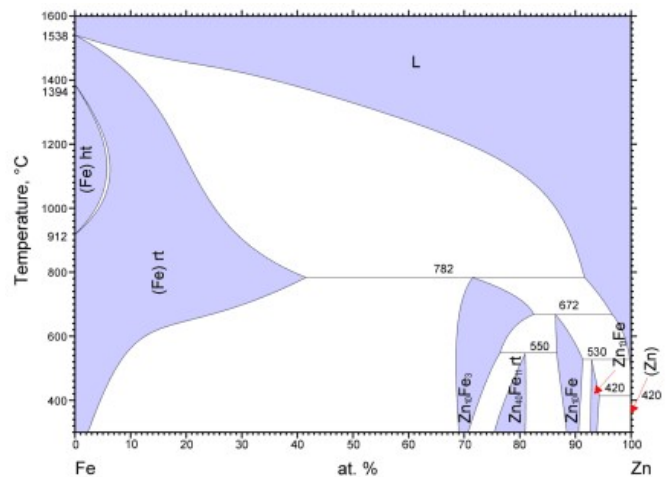
Table 1. Technical characteristics of the continuous galvanizing line studied

Technical specifications	Technical specifications
Zinc pot capacity	320 t
Fe-Zn pot capacity	280 t
Annual production capacity	280.000 t
Thickness range	0,25 a 2,00 mm
Width range	700 a 1500 mm
Galvanized coating	30 a 200 g/m ² /face
Fe-Zn coating	55 a 90 g/m ² /face
Maximum oven temperature	Preheating = 1250 ⁰ C and Soaking = 900 ⁰ C
Shielding gas	25%H ₂ e 75% N ₂
Max speed	180 m / min
Nominal production	26.8 t (0.38 x 1000 mm)
Maximum weight	40 t
Line length	282 m

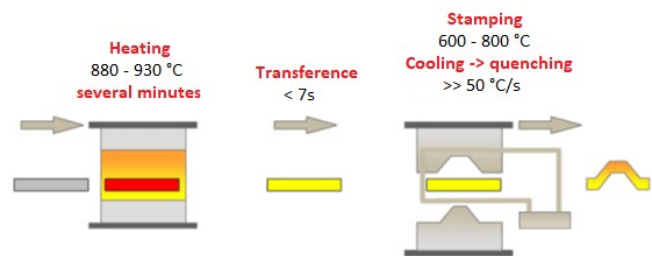
Galvanizing is the hot dip galvanizing process, which consists of immersing a steel sheet in a container with molten zinc at 460°C. The thickness is determined by a system of air knives, which affect the zinc fluid on the sheet, controlling the desired zinc layer for that application or technical standard.

Steel for hot stamping: The conventional cold stamping process of high strength steels is generally limited to the production of parts with relatively simple geometries due to limited formability and difficulties in geometric control associated with springback. High stamping forces, large geometric distortions and excessive tool wear are consequences of the high resistance to deformation of the material. For these applications, a boron-alloyed steel with Fe-Zn diffusion coating was developed. This steel is designed to be heat treated followed by a tempering operation during the stamping operation. The simultaneous stamping and tempering process is often used in parts that require high mechanical resistance and a great potential for weight reduction. This process is commonly called hot stamping or press hardening. The final mechanical characteristics allow a significant weight reduction per piece (up to 50% compared to a standard high resistance steel). The high elastic limit, obtained after heat treatment, is suitable for automotive components with anti-intrusion function, such as front and rear bumper bars, door reinforcements, floor, roof and B-pillar. boron steel from this research work for the development of the boron steel alloy and suitability for the steelmaking processes in the LD melt shop, such as chemical reactions and ladle metallurgy, continuous casting to control the level of the mold, control of the level of inclusions and solidification, hot rolling to dissolve the formed particles and thermomechanical control of the process, in chemical pickling the formation of the type of scale (oxides) on the surface of the hot rolled sheet, control of the hardening degree in cold rolling and temperature control of soak in annealing on continuous galvanizing line.

Metal Coatings: Aluminized metal coatings were evaluated, with different levels of alloying element (Si), and zinc coatings, such as pure Zn (galvanized-GI), alloyed with Fe (GA), and those with additions of Al, Mg, Mn, Cr and Cu, all in different concentrations. To determine the melting temperature of each of the alloys, together with the intermetallic phases likely to be formed during the solidification of the coating, the Thermocalc software was used. For each of these coatings, a specific processing cycle for CGL was developed, with optimized parameters to guarantee the surface quality of the coating and its good performance in hot forming application. Of the coatings evaluated, the one that presented the best results in terms of quality and performance, associated with the ease of producing it with the minimum of adaptations in the CGL, was the GA. For this steel, new simulations were carried out in wider ranges and narrower variations, both of the galvannealing cycles and of the heat treatment of austenitization and hot forming, aiming to adjust the qualities of the coating and steel to the applications of the automotive industry.

**Figure 1. Fe-Zn Diagram**

Hot Stamping: The hot stamping principle is directly related to the opportunities offered by the chemical composition of boron alloyed steels due to the robustness of the process window for the quenching operation. The 22MnB5 steel has a microstructure composed of ferrite-pearlite with a resistance limit of approximately 600 MPa. After the part is hot stamped, the microstructure obtained is predominantly martensitic and with an increase of up to 250% in the resistance limit. The hot stamping process starts with the austenitization of the blank (or with the pre-deformed part in the case of an indirect operation), usually in a continuous heating furnace for 4 to 10 minutes at temperatures between 880-930°C. This procedure creates a homogeneous austenitic microstructure. The blank is then quickly transferred to a press, with cooling systems integrated into the stamping tool, through an automatic transfer system, as shown in Figure 2.

**Figure 2. Schematic representation of the steps involved in the hot stamping process**

Parameters such as transfer time between the oven and the press must be carefully controlled in order to avoid possible reductions in the material's stamping capacity, associated with the localized occurrence of phase transformation during stamping, leading to discontinuities in the material's behavior, potential location of deformation and high friction in the bending regions generating tool wear. At high temperatures, between 650 and 900°C, the material has excellent formability and the part can be stamped in complex geometries in just one operation. Tempering preferably occurs after stamping, with the tool closed, thus avoiding localization of deformation due to localized hardening due to the presence of martensite. As a result of the microstructural change, it is possible to obtain parts with a resistance limit greater than 1500 MPa. The Fe-Zn coating, which during the austenitizing heat treatment transforms into alpha Fe phases, prevents oxidation and decarburization of the metal. Because the part is stamped at high temperatures and remains trapped inside the tool during the cooling step, the springback effect is minimized.

Definition of hot stamping conditions: During hot stamping processing, you must ensure that the final microstructure is 100% martensitic, not showing any diffusional microstructure such as pearlite, bainite and ferrite. In Figure 3, the regions where the hot

stamping process must be located can be seen. There is a region corresponding to stable austenite (ferrite/pearlite), in which phase transformation does not occur as a function of time. There is also a region corresponding to unstable austenite (bainite). It is in this region that the piece is stamped and, consequently, there is great interest in its characterization. As can be seen in Figure 3, to avoid bainite transformation, the cooling rate must be at least 30 °C/s. This critical cooling speed allows obtaining an entirely martensitic final microstructure. Finally, they have whether a region corresponds to a martensitic microstructure obtained during the quenching phase inside the stamping tool.

diffusional system is justified by the higher percentage of iron present in it, causing the melting point of the coating to increase and the time required for the complete transformation of the coating to be smaller, thus reducing the possibility of occurrence of LME. Comparing the coating ZN50 and ZN80, it can be seen that one has twice the layer thickness than the other, however, with similar iron percentages as listed in Table 4.

Hot Stamping Process during Material Approval period: The material approval process in automotive stamping involves an evaluation of mechanical and microstructural properties before and

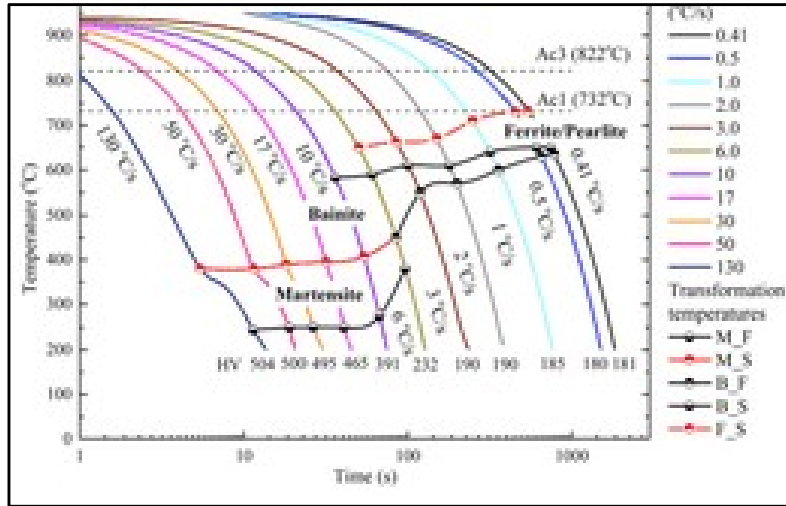


Figura 3. Continuous cooling transformation diagram of the 22MnB5 steel

Table 2. Chemical composition of CSN boron steel in mass percentage

C		Si		Mn		Mo + Cr		Ti		Al		B		S + P		OHN
Min	Max	Min	Max	Min	Max	Min	Max	Min	Max	Min	Max	Min	Max	Min	Max	Max
0,19	0,3	0,12	0,35	1	1,41	0,1	0,22	0,02	0,075	0,015	0,065	0,00015	0,00038	0,0002	0,0003	< 8 ppm

Table 3. Mechanical properties of boron steel in the as-received state (Uniaxial Test - Transverse Direction)

YL (MPa)	YS (MPa)	%Al 50 mm	R	n	Dureza
417	604	20	0,91	0,18	-

Table 4. Chemical composition of Fe-Zn diffusion system coatings

	% weight of the element		
	%Fe	%Al	%Zn
ZN50	10,2	0,1	89,7
ZN80	9,4	0,1	90,5

MATERIALS AND METHODS

The material evaluated in this work is a boron-alloyed steel industrially dedicated to hot forming, available from Companhia Siderúrgica Nacional (CNS). The chemical composition of the sample is shown in Table 2. Regarding the mechanical properties, this steel presents Yield Limit (YL) and Yield Strength (YS) values around 400 MPa and 600 MPa, respectively, as can be seen in Table 3. Samples coated with 2 different layer weights were developed. Layers coated with a range of 45 to 55 g/m²/face are called ZN50 and layers coated with a range of 70 to 90 g/m²/face are called ZN80. Table 4 presents the specifications of the layers, comparing the ZN50 and ZN80 coating. Two coating layers of the Fe-Zn diffusional system were evaluated, called ZN50 and ZN80, which respectively present 45 to 55 g/m²/face and 70 to 90 g/m²/face. Figure 4 shows the thicknesses of the coatings and the percentages of Fe and Zn present in both coatings in the state as annealed and galvanized, that is, without any heat treatment after hot-dip galvanizing. The Fe and Zn contents are represented from the distance of the substrate to the surface of the sample. The choice of coating for the Fe-Zn

after hot stamping. From the part under study (bumper reinforcement). 25 sketches of each coating, ZN50 and ZN80, were stamped and characterized for the evaluation of mechanical properties, microstructures formed for comparison purposes with samples obtained in laboratory scale. The stamping conditions were:

- Draft temperature: 900 °C
- Transfer time: 4s
- Ambient temperature: 25°C
- Stamping speed: 36 mm/s
- Quench time: 10 s
- Cooling rate: 50°C/s

To evaluate these properties, specimens with a measurement base of 50 mm were made from samples taken from the wall of the stamped part, according to the scheme in Figure 5 (a) and (b), as well as for hardness measurements, analysis of the coating and occurrence of cracks. Test requirements are described in Table 5.

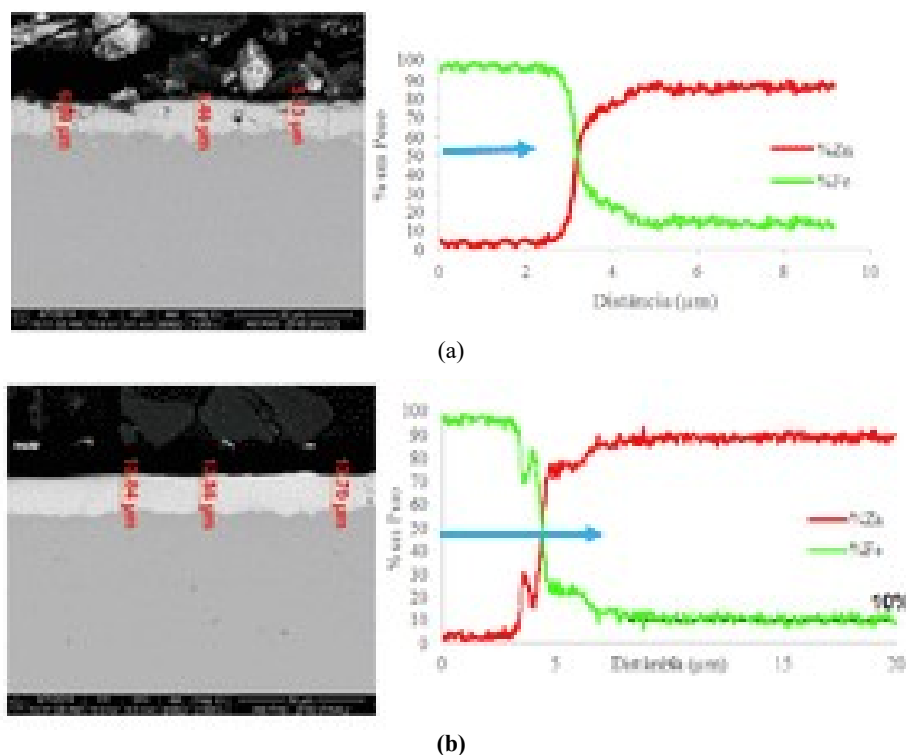


Figure 4. Characteristics of boron steel coatings before the hot stamping process: (a) ZN50 and (b) ZN80

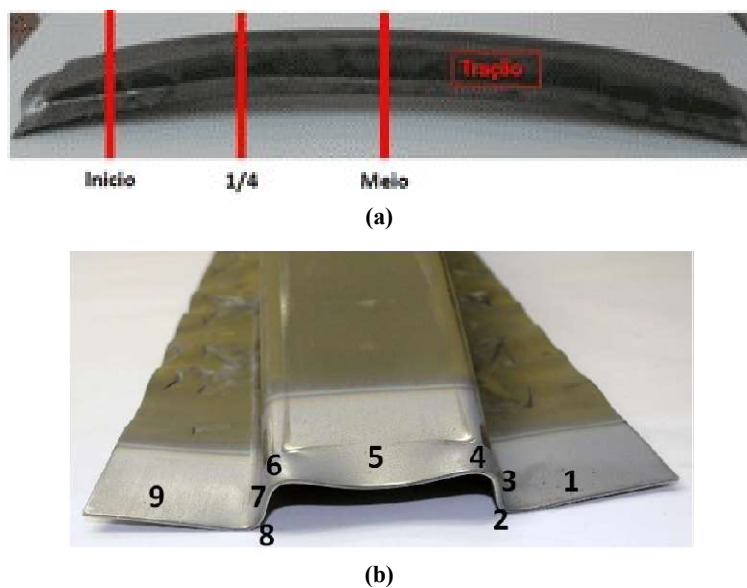


Figure 5. In (a) sampling scheme of tensile specimens and indication of sections analyzed for hardness, coating and microstructure evaluations in both coatings, in (b) regions of each area analyzed for both coatings

The samples coated with 2 different layer weights (ZN50 and ZN80) were subjected to different thermal treatments, varying the residence time at 900 °C. These samples had dimensions of 225 x 1,240 mm; in which they were hot stamped with Joule heating on an industrial scale in order to verify the non-occurrence of Liquid Melting Embrittlement (LME) in the prototype part and to evaluate the coating with Fe-Zn diffusional system.

RESULTS AND DISCUSSIONS

The results referring to the behavior of the steel are presented, namely, mechanical properties in uniaxial tension and microhardness measurements only in the 1/4 region for the two coatings. Based on Table 6, it can be inferred that the mechanical property values, after hot stamping, are in accordance with the technical specification of an automobile manufacturer, called company “Z” used as a technical

reference for application/use. The yield strength (YS) and resistance limit (RL) properties reached values greater than 1 GPa, with reasonable total elongation for a 100% martensitic microstructure. This level of resistance accredits and authorizes car manufacturers to replace cold-stamped parts that today have greater thicknesses, such as, for example, 2.80 mm, for less thick parts, thus reducing the mass of vehicles and even improving application/usage performance simultaneously. The Vickers microhardness (HV) measurements were performed on the 1/4 section of the part and are presented in Table 7. The average values obtained from three measurements are in line with what is expected for the martensitic microstructure, which is the objective of the hot stamping. In order to verify whether the entire piece had a martensitic microstructure, the nine regions of the pieces were evaluated and the results are shown in Figure 6. It is possible to state that most of the microstructures formed in the different regions for the piece coated with ZN50 present matrix mostly composed of martensite.

Table 5. Test Requirements for Material Approval (Bumper Reinforcement)

Evaluation	Test Method	Requirement
Mechanical Resistance (MPa)	Traction Tests	1280 – 1690
Flow (MPa)		950-1250
Elongation %(Lo=50mm)		≥ 5%
Thickness	Controlled in 4 zones, analysis in 1 point in each zone	Tolerance 20% smaller than the nominal thickness
Vickers hardness	3 points in each position, measure along the thickness	400 a 520 HV10
Rockwell hardness	3 points at each position, measure along the surface of the sample (removing coating)	40,8 a 50,5 HRC
Microstructure	Optical Micrograph 500x, etching Nital 4%.	It must have a 100% tempered martensitic structure.
Coating Layer Thickness	Optical Micrograph 500x	
	Total Coating Thickness	30 – 50 µm
	Diffusion Layer Thickness	≤ 16 µm
Evaluation	Test Method	Requirement
Mechanical Resistance (MPa)	Traction Tests	1280 – 1690
Flow (MPa)		950-1250
Elongation %(Lo=50mm)		≥ 5%
Thickness	Controlled in 4 zones, analysis in 1 point in each zone	Tolerance 20% smaller than the nominal thickness
Vickers hardness	3 points in each position, measure along the thickness	400 a 520 HV10
Rockwell hardness	3 points at each position, measure along the surface of the sample (removing coating)	40,8 a 50,5 HRC
Microstructure	Optical Micrograph 500x, etching Nital 4%.	It must have a 100% tempered martensitic structure.
Coating Layer Thickness	Optical Micrograph 500x	
	Total Coating Thickness	30 – 50 µm
	Diffusion Layer Thickness	≤ 16 µm

Table 6. Mechanical properties in uniaxial traction

Before hot stamping			After hot stamping		
Technical specification company "Z"		BZN boron steel of this research project	Technical specification company "Z"		
			ZN50	ZN80	
RL (MPa)	500 min	604	RL (MPa) = 1300-1650	1510	1640
YS (MPa)	300 min	417	YS (MPa) = 950-1250	1040	1080
%Al total 50 mm	15 min	20	%Al total 50 mm	5 min	5,6
					6,5

Table 7. Hardness of each region for section 1/4 of the piece

Hardness (HV) - standard deviation									
Region	1	2	3	4	5	6	7	8	9
ZN50	488-4	497-5	474-9	498-12	484-8	465-9	504-7	501-11	495-12
ZN80	495-8	480-12	470-10	499-11	501-10	505-10	488-11	490-13	494-11

With the exception of region 7, located at the lower radius of the wall of the part, where there is greater difficulty in heat exchange due to the contact pressure of the tool. Although this region has not been completely transformed into martensite, the microhardness value measured in this region is considered satisfactory, being 504HV. In order to verify whether the entire piece had a martensitic microstructure, the nine regions of the pieces were evaluated and the results are shown in Figure 6. It is possible to state that most of the microstructures formed in the different regions for the piece coated with ZN50 present matrix mostly composed of martensite. With the exception of region 7, located at the lower radius of the wall of the part, where there is greater difficulty in heat exchange due to the contact pressure of the tool. Although this region has not been completely transformed into martensite, the microhardness value measured in this region is considered satisfactory, being 504HV. In Figure 7, the microstructures of the stamped part with the ZN80 coating are shown. The part coated with the ZN80 coating, presented a 100% martensitic microstructure and, homogeneously, in all regions, thus achieving the main objective of obtaining a part composed of 100% martensitic structure. The difference in homogeneity between stamped parts with ZN50 and ZN80 coatings may not be related to the type of coating, but the temperature of the stamping tool during hot forming on an industrial experiment scale, since with the increase in the amount of stamped parts it is expected that there will be losses in the cooling capacity, mainly in wall regions. As with the microstructures, the coatings were also evaluated in relation to the enrichment that occurred during stamping in an industrial pilot environment and are presented below. The analysis identifications follow the previous item, however all sections of the stamped part were analyzed here, beginning, 1/4 and a half for all

regions from 1 to 9. EDS and LineScan values are presented for the percentages of Fe and Zn, in order to verify and confirm the complete transformation of the coating into an Fe- α phase. The beginning section of the piece is presented, in different regions, according to its geometric mode. Figure 8 shows the radius region, Figures 9 and 10 show the flat and wall regions, respectively. As regions 2, 3, 7, and 8 are critical for the occurrence of LME, since they comprise regions of radius and wall, and those of radius were analyzed on the surface that comprises the tensile stresses, that is, the external radius. As can be seen in Figure 8, the radius regions showed total enrichment of the coating, with percentage values of Fe greater than 56% (Pt1). The cracks presented in the coating did not have liquid zinc inside, and the cracks stopped propagating when they reached the substrate. Analyzing Figure 9, which are derived from wall positions, a lower intensity of cracks can be observed, but as with the rays, the entire coating was transformed into Fe- α (Pt1), probably being solid at high temperatures.

Figure 10 presents the results for the wall regions, where the material is stretched at values below 10%, which justifies the low incidence of cracks in the coating. Also, as in the radius and plane regions, the wall region also presented a 100% transformed coating with Fe percentages above 60% (Pt1). Therefore, it can be concluded that in all regions of the initial section, the coating showed an enrichment of Fe in the zinc layer capable of transforming the coating into a solid iron solution rich in zinc, Fe- α , with percentage values of Fe of the order of 60%, validating the parameterization carried out experimentally. However, some points presented a thin layer, of nanometric order rich in zinc, approximately 74% zinc.

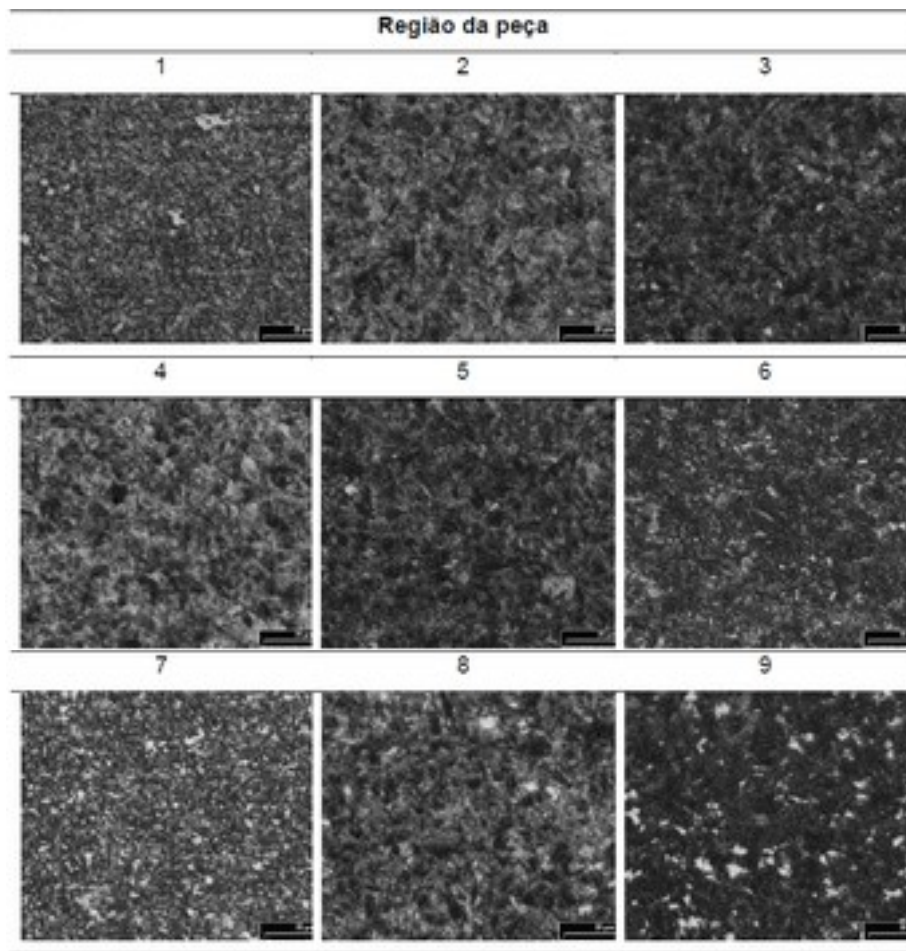


Figure 6. Microstructures formed on the part substrate cooled above 30 °C/s: regions 1 to 9 in the 1/4 section for the ZN50 coating. 1000x magnification. Nital 2%

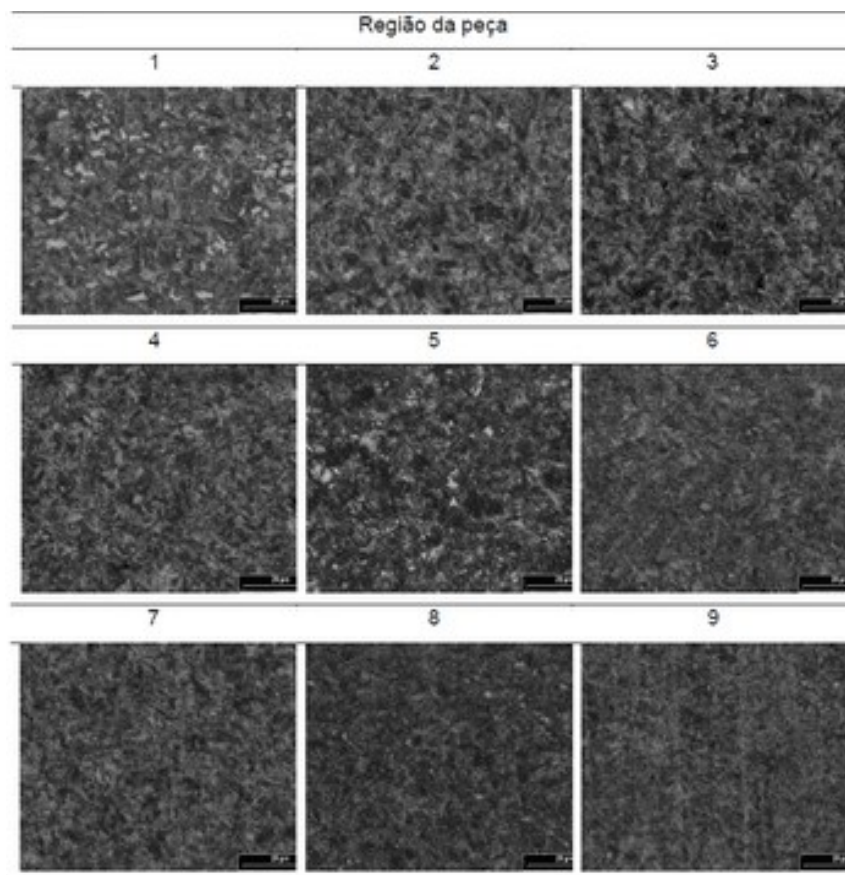


Figure 7. Microstructures formed on the substrate of the part cooled above 30 °C/s: regions from 1 to 9 in the 1/4 section for the ZN80 coating. 1000x magnification. Nital 2%

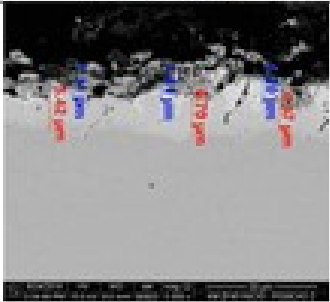
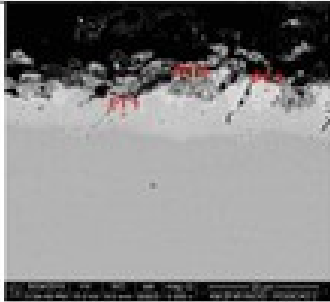
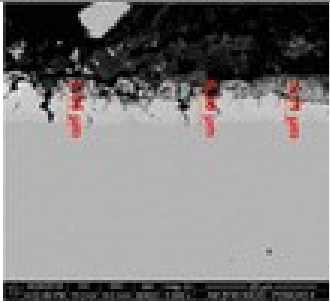
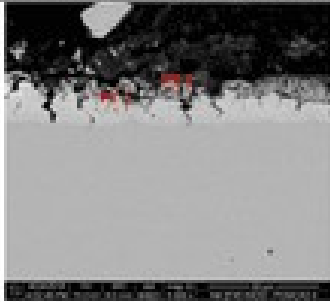
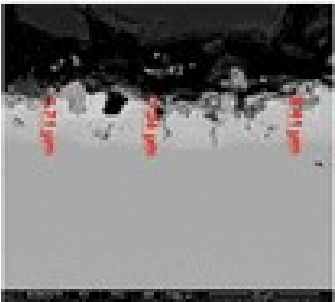
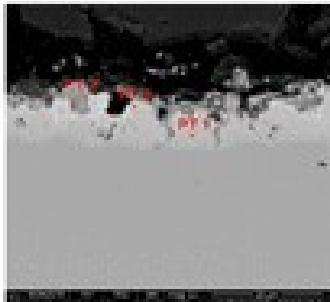
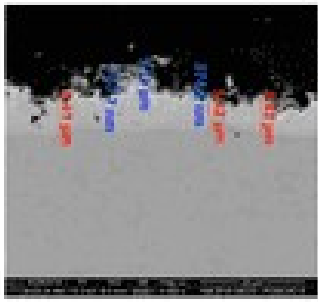
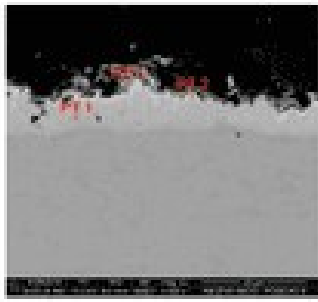
	Micro-estrutura do Revestimento	Análises de EDS	Valores das Análises de EDS
2			Pt1 %Fe 61,00 / %Zn 39,00
			Pt2 %Fe 25,88 / %Zn 74,12
4			Pt1 %Fe 64,56 / %Zn 35,44
			Pt2 %Zn 73,70 / %O 18,48 / %Fe 6,03 / %Mn 1,33
(a)			
6			Pt1 %Fe 56,17 / %Zn 43,83
			Pt2 %Zn 78,58 / %O 14,97 / %Fe 4,67 / %Mn 1,21
8			Pt1 %Fe 62,26 / %Zn 37,74
			Pt2 %Fe 27,18 / %Zn 72,82
			Pt3 %Zn 73,51 / %O 11,80 / %Fe 13,10 / %Mn 0,74
(b)			

Figure 8. Microstructure and EDS of the Coating - Home Section - ZN50, radius regions (2, 4, 6 and 8). In (a) regions 2 and 4 and in (b) regions 6 and 8

In addition, in none of the regions analyzed were any cracks attributed to the LME evidenced. Some cracks were observed in regions 2, 3, and 4, respectively, radius, wall and radius regions, in which theoretically the material is more stressed by flexion and friction effects.

These cracks are not of the LME type, as they only occurred in the coating, not penetrating the substrate (boron steel studied). Figures 11, 12 and 13 shows the microstructures and percentages of iron and zinc in the ZN80 coating at the beginning of the part, in order to

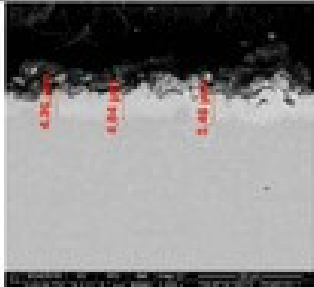
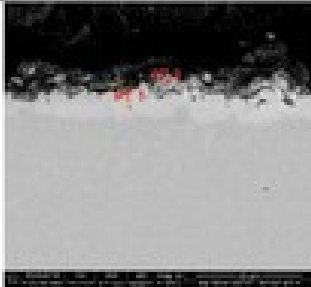
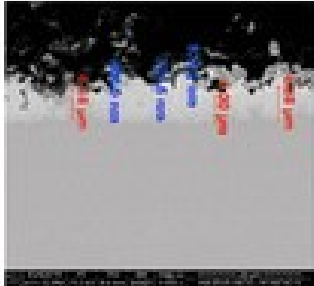
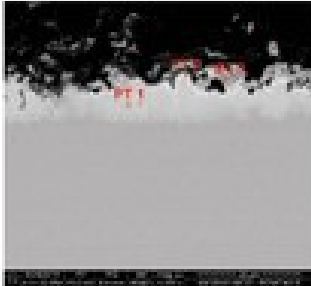
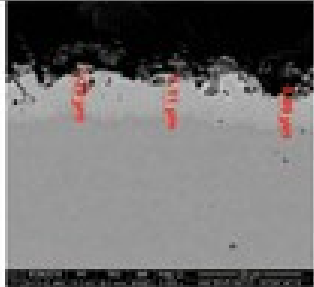
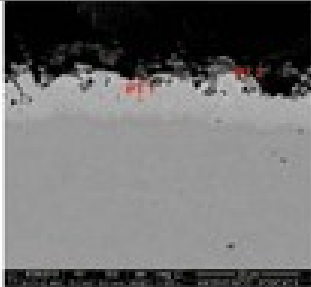
	Microestrutura do Revestimento	Análises de EDS	Valores das Análises de EDS
1			Pt1 %Fe 63,43 / %Zn 36,57 Pt2 %Zn 36,57 / %O 20,06 / %Fe 7,01 / %Mn 1,08
5			Pt1 %Fe 59,86 / %Zn 40,14 Pt2 %Fe 26,62 / %Zn 73,38 Pt3 %Zn 70,32 / %O 18,24 / %Fe 8,89 / %Mn 1,81
9			Pt1 %Fe 60,64 / %Zn 39,36 Pt2 %Zn 76,15 / %O 14,68 / %Fe 6,46 / %Mn 1,60

Figure 9. Microstructure and EDS of the Coating - Home Section - ZN50, flat regions (1, 5, 9)

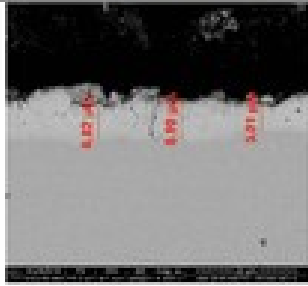
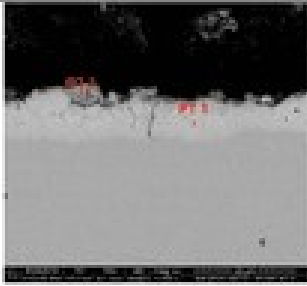
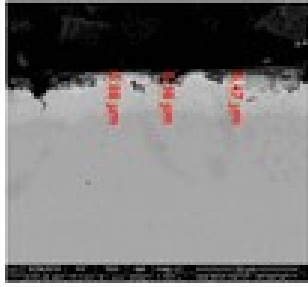
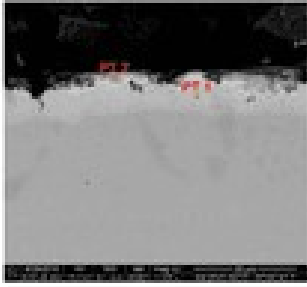
	Microestrutura do Revestimento	Análises de EDS	Valores das Análises de EDS
3			Pt1 %Fe 64,02 / %Zn 35,98 Pt2 %Zn 66,08 / %O 17,30 / %Fe 14,85 / %Mn 1,31
7			Pt1 %Fe 60,19 / %Zn 39,81 Pt2 %Zn 72,51 / %O 16,82 / %Fe 5,53 / %Mn 4,75

Figure 10. Microstructure and EDS of the Cladding - Home Section – ZN50, wall regions (3 and 7)

identify whether the entire layer was enriched with iron and whether there was no occurrence of LME-type cracking. Some images appear to have a porous appearance, this was due to contamination of the alcohol used for polishing, however the EDS analysis confirmed the percentages present in these phases without problems.

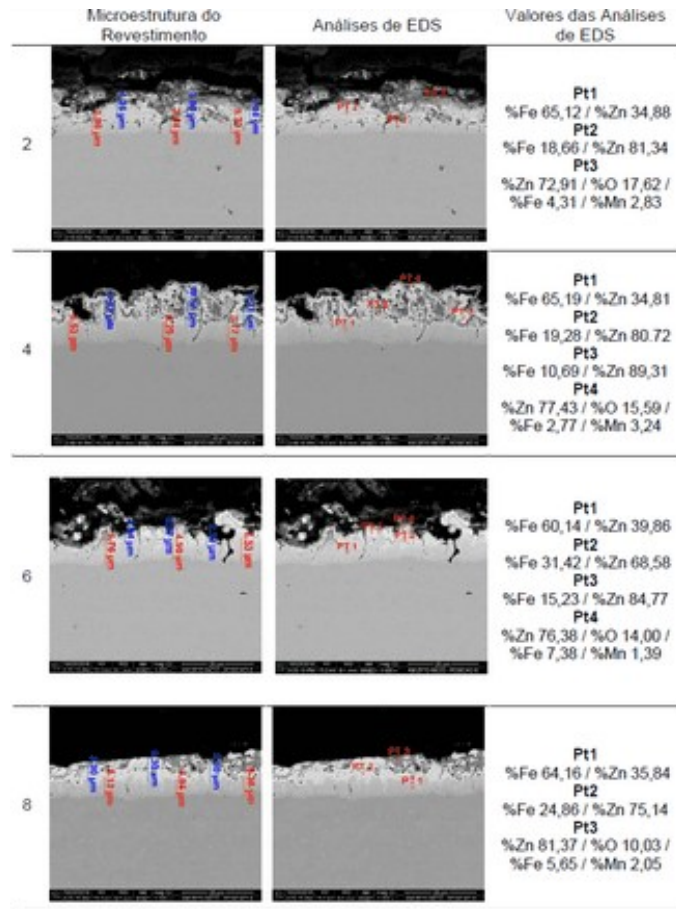


Figure 11. Microstructure and EDS of the Coating - Start Section - ZN80, radius regions (2,4,6 and 8)

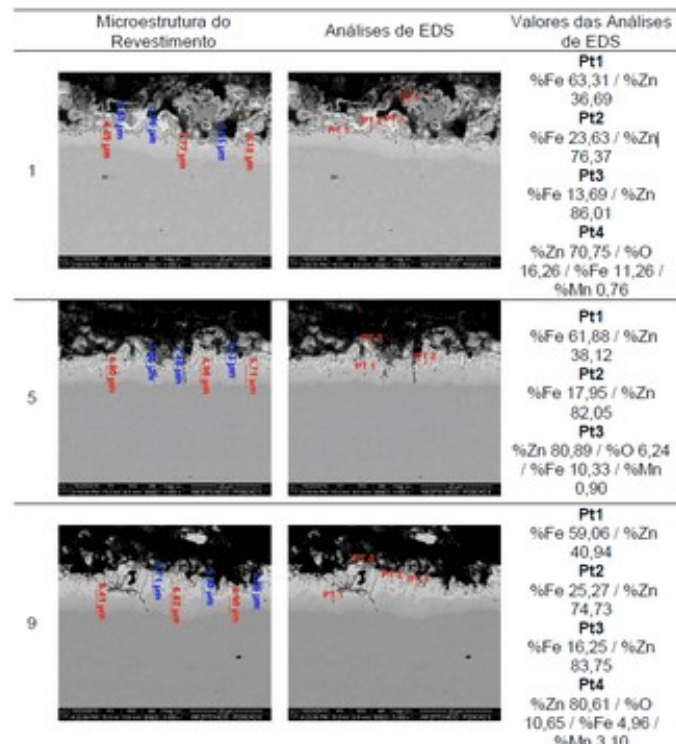


Figure 12. Microstructure and Coating EDS - Start Section - ZN80, flat regions (1,5 and 9)

According to Figure 12, it can be observed that the behavior in relation to the enrichment of Fe in the Zn-Fe layer for ZN80 was different. Not all of the coating layer was transformed (half), but even so cracks occurred crossing the Fe- α layer, but not penetrating the steel. In Figure 13, the results in the flat regions are presented, and as expected, part of the coating was transformed into Fe- α with percentages of Iron greater than 54% (Pt1), with the presence of cracks that are not of the LME type.

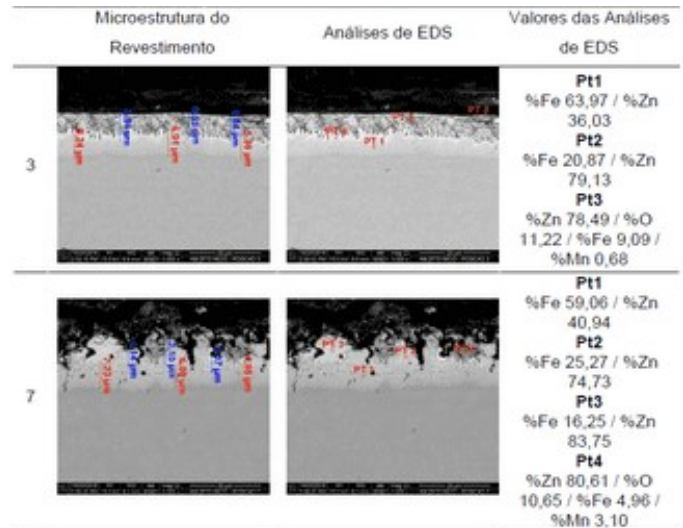


Figure 13. Microstructure and EDS of the Cladding - Start Section - ZN80, wall regions (3 and 7)

Based on the results of the initial section, it can be seen that there was no complete transformation of the ZN80 coating into the Fe- α phase, only part of the coating had an iron percentage greater than 54%, about 50% of the layer, and from 3 to 5 μm still have a high percentage of zinc, around 70 to 80%. According to GHAMBARI et. al. (2015) this fact would be enough to cause LME-type cracks, however, no crack was found that reached the steel, as can be seen in regions 4, 5, 6, 7, and 9, which comprise several regions such as radius, wall and flat. This fact may be linked to the level of stretching that the studied part presents, because higher levels of stretching can cause a greater occurrence of cracks, causing some to reach the substrate.

CONCLUSIONS

- From experiments on Fe diffusion in the coating, on a laboratory scale, it was possible to obtain results very close to those measured on stamped parts, particularly in the ZN50 coating, for which, contrary to expectations, the complete transformation of the coating was observed in the Fe- α phase, during the heating step of the metallic blank under high rates. Demonstrating that it is not necessary to soak at 900 °C, allowing reductions in time and cost of the process. On the other hand, the transformation of the ZN80 coating into Fe- α is complete only after a soaking time of 23 seconds at 900 °C;
- Subsidies were developed for the development of the process and the construction of the new manufacturing cell for hot stamping with Joule heating, with the opportunity to obtain a patent for the manufacturing process of hot stamping with Joule heating.

REFERENCES

NAKANO, J.; MALAKHOV, D.V.; PURDY, G.R.A crystallographically consistent optimization of the Zn-Fe system, CALPHAD: Comput. Coupling Phase Diagrams Thermochem, v. 29, p. 276-288, 2005.

- GHAMBARI, Z. N.; SPEER J. G.; FINDLEY, K. O. Coating Evolution and Mechanical Behavior of Zn-Coated Press-Hardening Sheet Steel. In Proceedings of Hot Sheet Metal Forming of High-Performance Steel, 5^o International Conference, p. 355–362, 2015.
- CUI, J. et al. Predictions of the mechanical properties and microstructure evolution of high strength steel in hot stamping. *Journal of Materials Engineering and Performance*, v. 21, p. 2244-2254, 2012.
- DRILLET, P.; GRIGORIEVA, R. LEUILLIER, G. Study of Cracks Propagation Inside the Steel on Press Hardening Steel Zinc Based Coatings. Galvatech'11 Conference, Genova, 2011.
- IKEUCHI, K.; YANAGIMOTO, J. Valuation method for effects of hot stamping process parameters on product properties using forming simulator. *Journal of Materials Processing Technology*, v. 211, p. 1441-1447, 2011.
- JEON, Y. J.; SONG, M. J.; KIM, H. K.; CHA, B. S. Effect of hot-stamping process conditions on the changes in material strength. *International Journal of Automotive Technology*, v. 16, n. 4, p. 619-627, 2015.
- JIAN, B. et al, Impact of Nb Microalloying on the Hydrogen Embrittlement of Press Hardening Steel. In Proceedings of Hot Sheet Metal Forming of High-Performance Steel, 5^o International Conference, p. 65–74, 2015.
